$C^{13}(He^3,\alpha)C^{12}$ Reaction and Elastic Scattering of He^3 from C^{13} at 12, 15, and 18 MeV

E. M. KELLOGG* AND R. W. ZURMÜHLE
Department of Physics, University of Pennsylvania, Philadelphia, Pennsylvania
(Received 6 July 1966)

The $C^{13}(He^3,\alpha)C^{12}$ reaction was studied at 12, 15, and 18 MeV. Complete angular distributions of elastically scattered He^3 as well as those of α particles leading to the ground, 4.433–, 7.656–, 9.64–, 10.84–, 11.83–, and 12.71-MeV states were measured. A set of optical-model parameters that fits the elastic-scattering cross section of He^3 at all three energies was found with the HUNTER program. It shows only a slight negative energy dependence of the real well depth and a positive energy dependence of the imaginary well depth. Distorted-wave Born approximation (JULIE) analysis shows pickup of $l=1$ or 0 for all excepting the 9.64-MeV state, where $l=2$ is found. Relative spectroscopic factors were extracted.

INTRODUCTION

THE purpose of this experiment was to obtain more information on single-particle configurations involved in a single-neutron transfer occurring in the (He^3,α) transition between the C^{13} ground state and several states of C^{12}. The work of Bennett[1] on the $C^{13}(p,d)C^{12}$ reaction showed that the neutron pickup hypothesis was reasonable in giving agreement between his results and plane-wave Born approximation (PWBA) predictions, within the restrictions of the plane-wave theory. His work covered the ground- and 4.43-MeV-state transitions to C^{12} only. The $C^{13}(He^3,\alpha)C^{12}$ reaction has been observed by several workers[2–6] in the past. Most of these observations were of the transition to the ground state. The most systematic study was done by Deshpande.[6] He was able to measure complete angular distributions of the ground and 4.43-MeV states at energies up to 10.29 MeV.

The present work gives complete angular distributions for all states up to 12.71-MeV excitation in C^{12}, at bombarding energies up to 18.0 MeV, where the direct-reaction assumption should be more valid. In addition, the entrance-channel elastic-scattering angular distributions were measured in order to remove some ambiguity in DWBA analysis of the data. The DWBA calculations and resulting spectroscopic factors are discussed in some detail.

APPARATUS AND TECHNIQUES

The He^{3++} beam from the University of Pennsylvania Model EN Tandem Van de Graaff accelerator was used. Beam currents up to 0.14 μA were obtained at energies to 18.0 MeV. The spot size at the target was approximately equal to $\frac{1}{16}$-in. diameter. For the reaction measurements, targets of 60% C^{13} enrichment were adequate. These were self-supporting films of 100 to 150 μg/cm^2 and 0.5-in. diameter, mounted on 0.015-in.-thick tantalum sheet. The 40% impurity of C^{12} made these targets useless for the elastic-scattering measurements, since the elastic groups from the two different isotopes could not be resolved. Thus, a series of targets of 90% C^{13} enrichment were prepared. They were made by cracking enriched methyl iodide[7] onto a 1-mil Ni foil, and etching away the foil. Then the remaining carbon film was lifted from the surface of the etching solution, onto the tantalum target frame. Targets from 30 to 150 μg/cm^2 were made in this way.

The angular distributions were measured in vacuum using silicon solid-state detectors. The scattering chamber which the detectors and target were mounted in has been described elsewhere.[8] For the alpha-particle measurements, surface-barrier detectors with depletion depths from 150 to about 500 μ were used. The depletion depth was chosen to stop the C^{12} ground-state alpha group ($Q=+15.630$ MeV). This thickness would stop protons of only less than one-third the energy of the ground-state alpha group. In that way, protons were eliminated from the upper two-thirds of the spectrum. The required depletion depth was a function of the angle, because of kinematic effects. The pulses from each detector were fed into a Tennelec 100A preamplifier and from there went into a linear amplifier and into a TMC-4096 pulse-height analyzer, which stored the spectra from eight detectors simultaneously.

The elastic-scattering measurements required a particle identification system. A (dE/dx)-E detector telescope was used. It consisted of a 17-μ-thick silicon wafer fully depleted detector for the ΔE pulse, mounted in front of a surface-barrier silicon detector with a depletion thickness of 500 μ for the E pulse. The ΔE and E pulses were each fed through preamplifiers and amplifiers into the TMC-4096 pulse-height analyzer operating in the two-parameter mode.

* Present address: American Science & Engineering, Inc., Cambridge, Massachusetts.

[1] E. F. Bennett, Phys. Rev. **122**, 595 (1961).

[2] E. Almquist, D. A. Bromley, A. J. Ferguson, H. E. Gove, and A. E. Litherland, Phys. Rev. **114**, 1040 (1959).

[3] H. D. Holmgren, E. H. Geer, R. L. Johnston, and E. A. Wolicki, Phys. Rev. **106**, 100 (1957).

[4] R. Barjon, M. Lambert, and J. Schmouker, J. Phys. Radium **21**, 356 (1960).

[5] H. D. Holmgren and E. A. Wolicki, in *Proceedings of the Rutherford Jubilee International Conference 1961*, edited by J. B. Berks (Academic Press Inc., New York, 1961).

[6] V. K. Deshpande, Nucl. Phys. **70**, 561 (1965).

[7] G. C. Phillips and J. E. Richardson, Rev. Sci. Instr. **21**, 885 (1950).

[8] R. W. Zurmühle, Nucl. Instr. Methods **36**, 168 (1965).

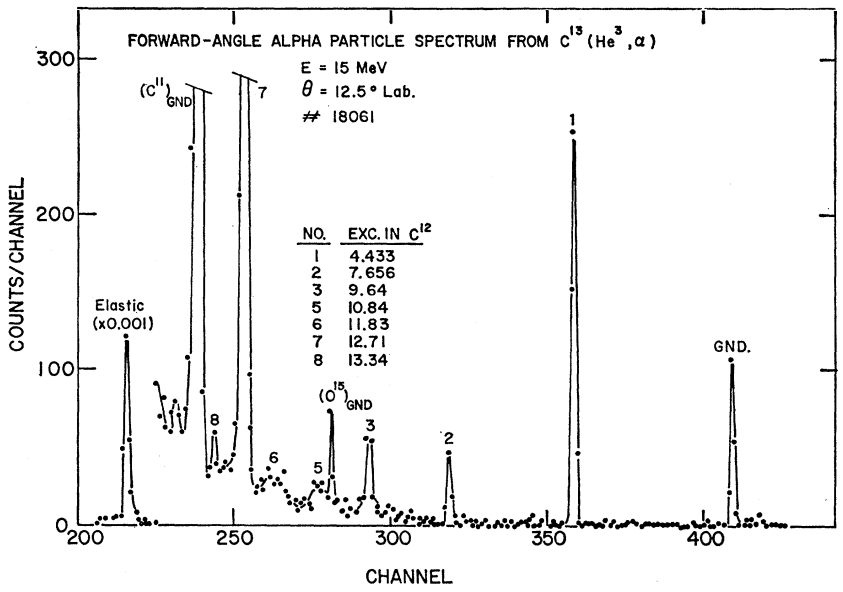

FIG. 1. Typical alpha-particle spectrum from $C^{13}(He^3,\alpha)C^{12}$ with a 60% enriched C^{13} target.

For the (He^3,α) reaction at angles between 5° and 175° eight counters were used simultaneously, mounted 10° apart. The 5° counter had a $\frac{1}{16}$-in.-diam round aperture and was equipped with an ORTEC pile-up rejection system. The 10° counter had a $\frac{1}{8}$ in.-diam round aperture and a pile-up rejection circuit. The rest of the counters had $\frac{1}{8}$ in. wide by $\frac{1}{4}$ in. high rectangular apertures. The $\frac{1}{8}$ in. horizontal limit (at a target-detector separation of 9 in.) was necessary to keep the energy width of a group due to angular extent of the detector small. A typical $C^{13}(He^3,\alpha)$ spectrum is shown in Fig. 1. The continuum whose upper limit is seen near the No. 2 group is from the breakup of C^{12} into $Be^8+\alpha$. Angular distributions could not be obtained on groups with Q values lower than that of group No. 7 ($Q=+2.92$ MeV) because of interference from other types of particles, and alphas from other reactions, such as $C^{12}(He^3,\alpha)C^{11}$, $Q=1.86$ MeV.

For the elastic scattering at angles from 5° to 30°, particle identification was not necessary, since the He^3 elastic peak dominates the spectrum. The high count rate at these angles required a reduction of beam current to 5×10^{-9} A in order to keep the errors in correcting for analyzer dead time low. The elastic-scattering measurements at angles greater than 30° required the particle identification technique described above. The two distinct peaks obtained for He^3 and He^4 are shown in Fig. 2. This shows a slice of the two-dimensional 64×64-channel memory field at constant E (i.e., pulses giving the same pulse height in the E detector). The He^3 elastic peak was distributed over several such slices at each angle and bombarding energy. The solid line in Fig. 2 is a visual fit to the data points. The elastic He^3 yield obtained above contained an unknown contribution from $C^{12}(He^3,He^3)C^{12}$ elastics because of the 10%

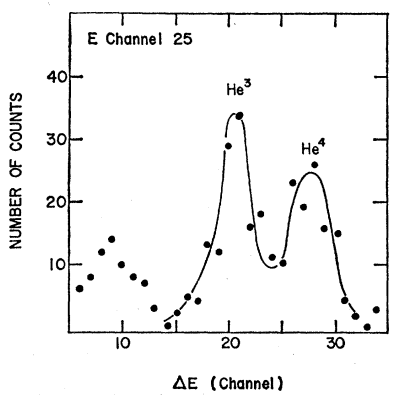

FIG. 2. dE/dx-versus-E data, used for the He^3 identification in the elastic scattering. The dE/dx counter was 17 μ thick. This slice of constant pulse height in the E counter is extracted from the complete two-dimensional spectrum.

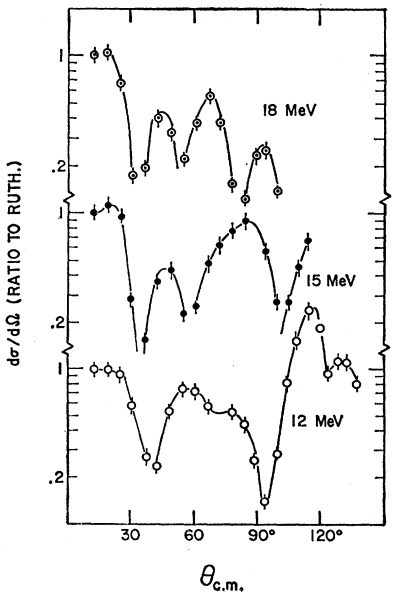

FIG. 3. $C^{12}(He^3, He^3)C^{12}$ elastic scattering expressed in terms of the Rutherford cross section. The points are the data. The curves are a visual fit, as no theoretical comparison was made.

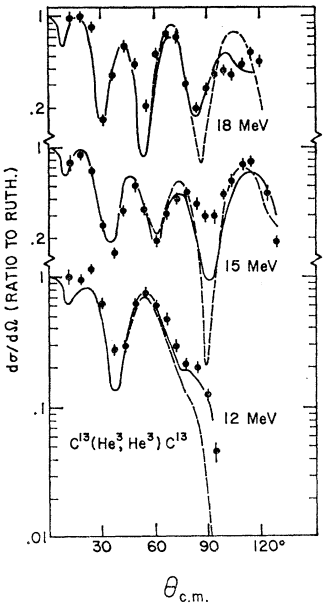

FIG. 4. $C^{13}(He^3,He^3)C^{13}$ elastic scattering expressed in terms of the Rutherford cross section. The absolute cross sections of the data (points) were normalized independently at all three energies by no more than 20% to give best agreement with HUNTER calculations (curves). The solid lines are calculations including $\mathbf{l}\cdot\mathbf{s}$ coupling. The broken lines are calculations without $\mathbf{l}\cdot\mathbf{s}$ coupling. The parameters are listed in Table I.

of C^{12} in the target. Therefore, it was necessary to measure the He^3 elastics from C^{12}. The results are shown in Fig. 3. This contribution was evaluated and subtracted out by measuring the elastic scattering of He^3 from C^{12} using a natural-carbon target.

The absolute cross sections were determined in the following way. The total number of beam particles was measured using a Faraday-cup beam stop (±5% error). The target thickness was measured by finding the energy loss of Am^{241} alphas in the target and using the known value of dE/dx in carbon for alpha particles (over-all error in target thickness estimated at ±10%). The solid angle subtended at the center of the target by the detector was calculated from the measured aperture size used on the detector and the target-detector distance, which is set by the location of the detector mounting holes in the scattering chamber (solid-angle error estimated at ±5%). The probable error in the absolute cross sections, due to these three sources of error, is then ±13%.

In the process of optical-model fitting with the HUNTER program, the data had to be renormalized in order to give a good fit at small angles, where the calculated cross section is insensitive to the choice of the parameters. The normalization factors were within 20% of unity. They were applied to the data shown in Fig. 4.

DATA ANALYSIS AND RESULTS

$C^{13}(He^3,He^3)C^{13}$ Elastic Scattering

The elastic-scattering data were fitted by the optical-model search program HUNTER. The optical potential used was

$$U=V(r)+V_{so}(r)\mathbf{l}\cdot\boldsymbol{\sigma}+i[W(r)+W_s(r)]+V_c(r),$$

with

$$V(r)=-V(1+e^x)^{-1},\quad x=(r-r_0A^{1/3})/a,$$

$$V_{so}(r)=V_{so}f_{so}(x),\quad f_{so}(x)=\left(\frac{\hbar}{M_\pi c}\right)^2\frac{1}{r}\frac{d}{dr}(1+e^x)^{-1},$$

$$W(r)=-W(1+e^y)^{-1},\quad y=(r-r_0A^{1/3})/b,$$

$$W_s(r)=r_4(d/dy)(1+e^y)^{-1},$$

$$V_c(r)=Z_aZ_Ae^2/r\quad\text{for}\quad r\geq r_cA^{1/3},$$

$$V_c(r)=\frac{Z_aZ_Ae_2}{2r_cA^{1/3}}\left(3-\frac{r^2}{r_c^2A^{2/3}}\right)\quad\text{for}\quad r\leq r_cA^{1/3}.$$

The normalized experimental data points and the curves calculated by HUNTER are shown in Fig. 4. The calculated cross-section was quite sensitive to the inclusion of V_{so}, as we see from the broken-line curves, with $V_{so}=0$. The parameters used in the calculations are given in Table I. The geometrical parameters are fixed and only V and W have an energy variation. This was prescribed in the final HUNTER search. The early searching without a spin-orbit term showed the sharp dip at about 90° to persist through variation of the geometry and other parameters. Values of 4.0, 6.0, 8.0, and 12.0 MeV for V_{so} were tried, with 6.0 giving the best fit. Various other regions of V were investigated, namely: 80, 120, and 250 MeV. None of these yielded fits as good as the 160 MeV well depth.

$C^{13}(He^3,\alpha)C^{12}$ Reaction

The angular distributions for the $C^{13}(He^3,\alpha)C^{12}$ reaction were measured at 12.0, 15.0, and 18.0 MeV. The alpha-particle groups leading to the ground, 4.433-, 7.656-, 9.64-, 10.80-, 11.83-, and 12.71-MeV excited states in C^{12} were measured from 5° to 175° (lab angles). No evidence was found for the excitation of a state of cross section >0.01 mb/sr at 10.1 MeV. The data points are shown in Fig. 5, together with DWBA calculations performed using the JULIE code[9] assuming a pickup mechanism. The general features of the data indicate that the reaction occurs by a direct process, shown by strong forward peaking. The backward peaking has been previously accounted for in calculations by using

TABLE I. Optical parameters for $C^{13}(He^3,He^3)C^{13}$ elastic scattering.

V (MeV)	W (MeV)	r_0 (F)	a (F)	r_g (F)	b (F)	r_c (F)	V_{so} (MeV)	He^3 lab energy (MeV)
156.	6.8	0.93	0.81	2.25	0.65	1.4	6	18.0
158.	6.75	0.93	0.81	2.25	0.65	1.4	6	15.0
161.	5.37	0.93	0.81	2.25	0.65	1.4	6	12.0

[9] R. H. Bassel, R. M. Drisko and G. R. Satchler, Oak Ridge National Laboratory Report No. ORNL-3240 (unpublished); R. H. Bassel (private communication).

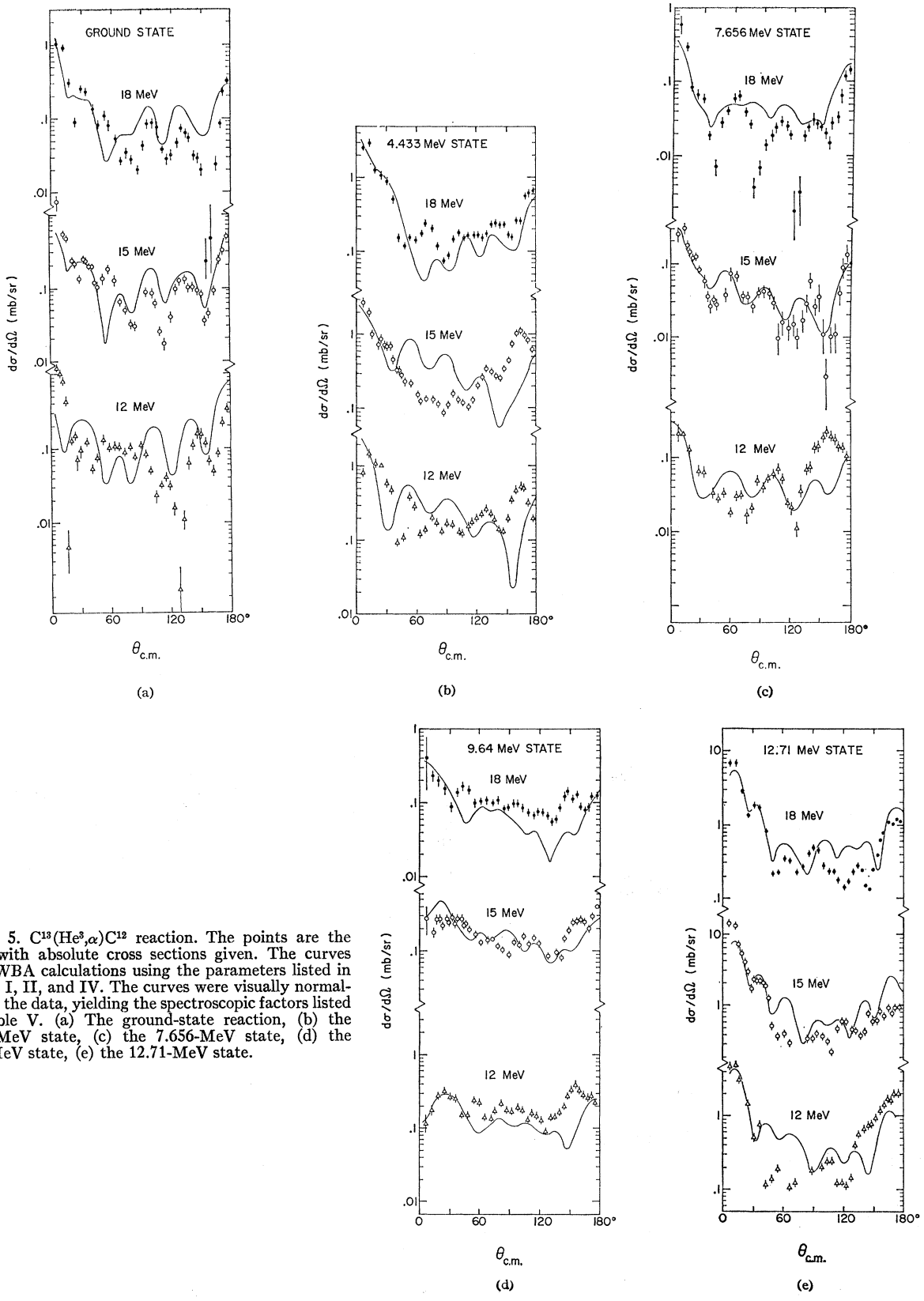

FIG. 5. $C^{13}(He^3,\alpha)C^{12}$ reaction. The points are the data, with absolute cross sections given. The curves are DWBA calculations using the parameters listed in Tables I, II, and IV. The curves were visually normalized to the data, yielding the spectroscopic factors listed in Table V. (a) The ground-state reaction, (b) the 4.433-MeV state, (c) the 7.656-MeV state, (d) the 9.64-MeV state, (e) the 12.71-MeV state.

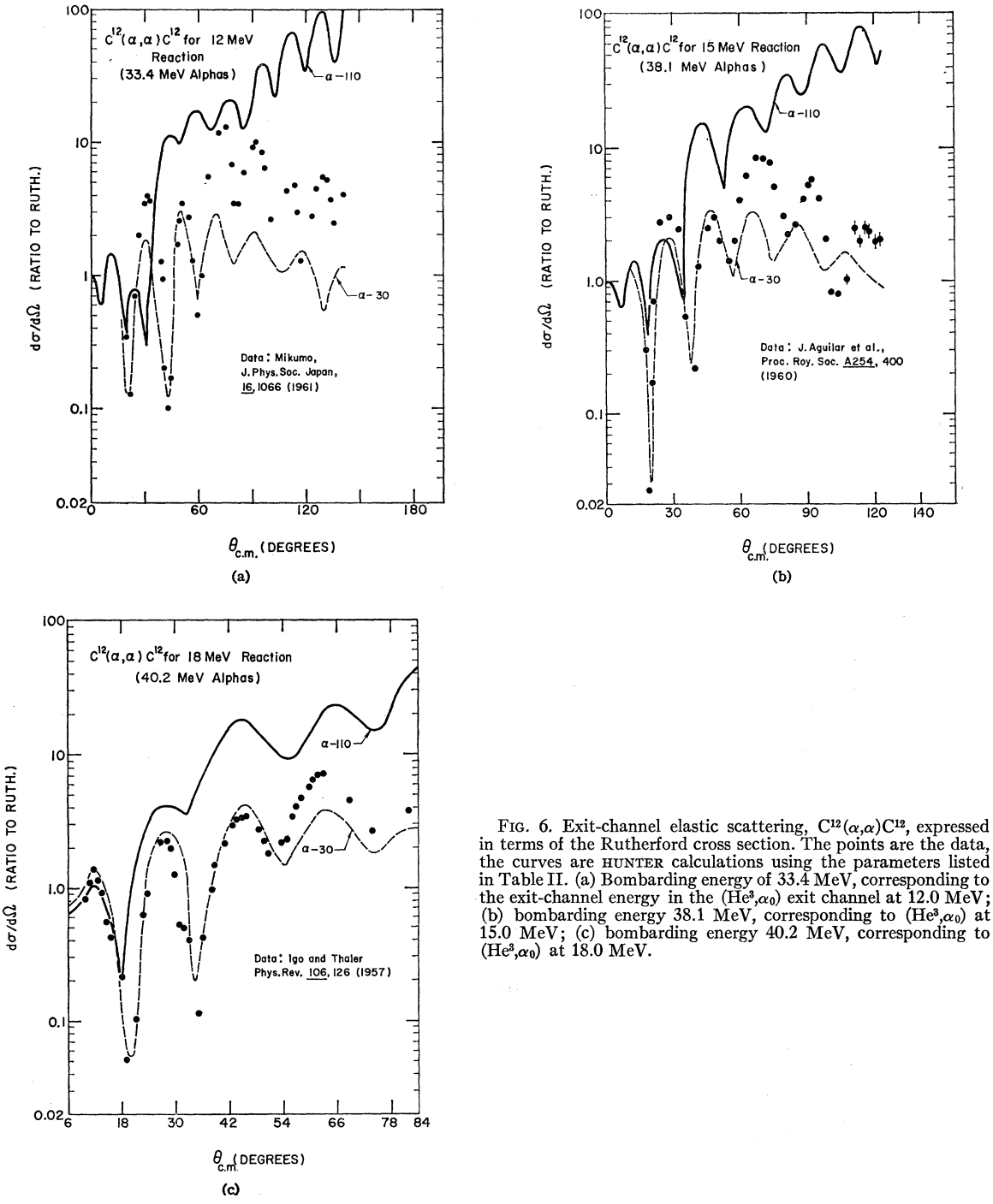

FIG. 6. Exit-channel elastic scattering, $C^{12}(\alpha,\alpha)C^{12}$, expressed in terms of the Rutherford cross section. The points are the data, the curves are HUNTER calculations using the parameters listed in Table II. (a) Bombarding energy of 33.4 MeV, corresponding to the exit-channel energy in the (He^3,α_0) exit channel at 12.0 MeV; (b) bombarding energy 38.1 MeV, corresponding to (He^3,α_0) at 15.0 MeV; (c) bombarding energy 40.2 MeV, corresponding to (He^3,α_0) at 18.0 MeV.

plane-wave theory, assuming that so-called "heavy-particle stripping" occurred as well.[10] It was not necessary to postulate such a process in the present analysis. The absolute values of the cross sections for the ground, 4.433-, and 7.656-MeV states at 12.0 MeV are lower than the results obtained by Deshpande[6] at 10.29 MeV by about a factor of 5.

[10] G. E. Owen, L. Madansky, and S. Edwards, Phys. Rev. 113, 1575 (1959).

Comparison of Exit-Channel Parameters and Scattering

In this reaction, there is a large amount of data available for the exit-channel elastic scattering, i.e., $C^{12}(\alpha,\alpha)C^{12}$. If one examines the data, it is found that

the angular distributions vary rapidly with bombarding energy. In fact, Carter, Mitchell, and Davis showed that there are strong resonances.[11] Thus, it is not clear whether a particular set of optical parameters derived from the exit-channel scattering data is appropriate for use in the JULIE calculations in the present case. In this study, we tried several sets of parameters, given in Table II. The α-30 set was obtained by Igo and Thaler[12] by fitting the $C^{12}(\alpha,\alpha)C^{12}$ elastic scattering data at 40.2 MeV, which is the energy corresponding to the exit-channel energy in the $C^{13}(He^3,\alpha)C^{12}$ reaction at 18.0-MeV He^3 energy. The other sets were obtained by Carter, Mitchell, and Davis[11] by fitting the exit-channel data at off-resonance energies.

Our energies of interest are shown in Table III.[13,14] The first column gives the He^3 bombarding laboratory energy; second, the corresponding laboratory energy to the (He^3,α) ground-state exit channel for $C^{12}(\alpha,\alpha)C^{12}$; third, the nearest laboratory energy at which experimental data are available for $C^{12}(\alpha,\alpha)C^{12}$ elastic scattering; fourth, the reference to the published data. It is interesting to compare the experimental data with the α-110 set of exit-channel parameters, and with the α-30 set obtained by fitting the 40.2-MeV data. Figure 6 shows the data, with the optical-model predictions from the α-110 set and the α-30 set. As expected, the α-30 set gives very good agreement at 40.2 MeV. The agreement deteriorates at the lower energies. The α-110 set gives only a qualitative agreement at 40.2 MeV, and at the forward angles at 38.1 MeV, but no agreement at 33.4 MeV. Figure 7 shows a fit of the $C^{13}(He^3,\alpha)C^{12}$ ground-state transition at 18 MeV, using the α-30 set. Except for the normalization of the calculated cross section, there are no free parameters in this fit. Both the forward and backward peaking of the angular distribution are well fitted. The structure between 60° and 120° is, however, not reproduced. The theoretical curve is much too smooth. A lower radial cutoff was applied to improve the agreement. The results are shown in Fig. 8. An almost equally good fit could be obtained with the α-110 potential, using a slightly different lower cutoff. In addition, this latter potential gave better results for most excited-state transitions. We feel that the better agreement of the alpha elastic-scattering data with the α-30 prediction is not a sufficient reason for preferring it in the DWBA calculation of transitions leading to excited states. We, therefore, used the α-110 potential in all our calculations.

TABLE II. Exit-channel optical parameters.

V (MeV)	W (MeV)	r_0 (F)	a (F)	r_g (F)	b (F)	r_c (F)	V_{so} (MeV)	r_4 (MeV)	Name
30.	10.	1.92	0.5	1.92	0.5	1.22	0	0	α-30
75.	0	1.77	0.6	1.77	0.6	1.22	0	16.	α-75
110.	0	1.87	0.5	1.87	0.3	1.22	0	16.	α-110
200.	0	1.97	0.5	1.87	0.3	1.22	0	16.	α-200

TABLE III. Exit-channel energies. E_0 is the lab energy for $C^{13}(He^3,\alpha)C^{12}$. E_{lab} is the lab energy required for $C^{12}(\alpha,\alpha)C^{12}$ to obtain the energy corresponding to the (He^3,α_0) exit channel. E_{expt} is the nearestl ab energy at which measurements of $C^{12}(\alpha,\alpha)C^{12}$ were done.

E_0 (MeV)	E_{lab} (MeV)	E_{exp} (MeV)	Reference
12	33.8	33.4	13
15	37.1	38.1	14
18	40.3	40.2	12

DWBA Calculations

Several variations on the standard JULIE calculation techniques are possible. Those investigated here are: The effective-binding-energy scheme, nonlocal potentials (using the FLANNEL FLURP[15] code), and the lower radial cutoff procedure (R_c).

The binding energy in the target nucleus of the neutron to be picked up must be included in the calculation. This is needed to specify the wave function of the neutron in C^{13}. The usual technique is to set the binding energy equal to the neutron separation energy. The separation energy is equal to the mass difference

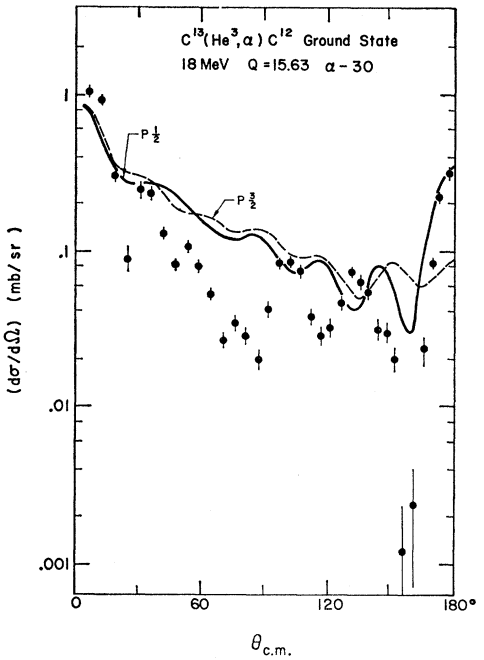

FIG. 7. The predictions of the DWBA calculation of the $C^{13}(He^3,\alpha)C^{12}$ ground-state transition at 18 MeV with α-30 potential. No radial cutoff is applied. The dashed curve represents the calculation for pickup of a $p_{3/2}$ neutron and shows the influence of the spin-orbit term in the He^3 optical potential on DWBA.

[11] E. B. Carter, G. E. Mitchell, and R. H. Davis, Phys. Rev. **133**, B1421 (1964).
[12] G. Igo and R. M. Thaler, Phys. Rev. **106**, 126 (1957).
[13] Takashi Mikumo, J. Phys. Soc. Japan **16**, 1066 (1961).
[14] J. Aguilar *et al.*, Proc. Roy. Soc. (London) **A254**, 400 (1960).
[15] R. H. Bassel (private communication).

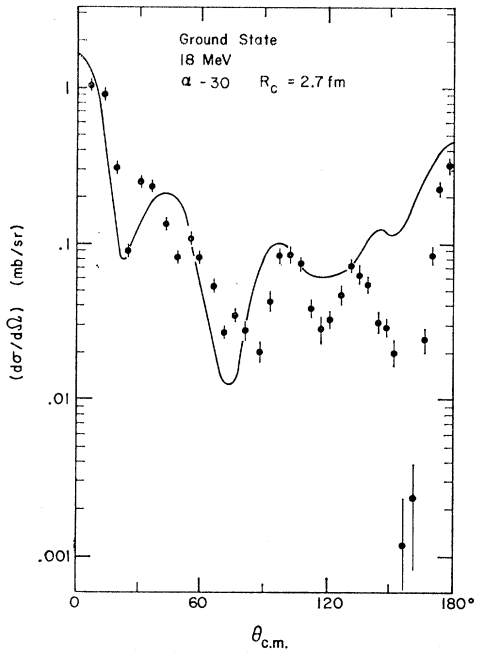

FIG. 8. The predictions of the DWBA calculation of the $C^{13}(He^3,\alpha)C^{12}$ ground-state transition at 18 MeV with α-30 potential and a lower radial cutoff $R_c=2.7$ F.

between $C^{12*}+n$ and C^{13}, with C^{12} in the excited state corresponding to the alpha-particle group observed in that case. In the effective-binding-energy scheme, another prescription is used. For example, we may look at a series of states of C^{12} which are all thought to be formed by the pickup of a neutron from the same orbital in C^{13}. We assign the same binding energy to the neutron in all these cases. This procedure was tried for the 4.433 and 12.71-MeV states in C^{12}, both of which are thought to be excited by $p_{3/2}$ pickup. The 4.433-MeV state was assumed to have the binding energy equal to the separation energy. The 12.71-MeV state was given the same binding energy as the 4.433-MeV state. The shape of the angular distribution for the 12.71-MeV state was changed little from the case when the separation-energy prescription was used. The absolute calculated cross section was increased by a factor of 7. The large size of the change was partly due to the use of a lower radial cutoff. The calculation is then very sensitive to the tail of the bound neutron's wave function which in turn is changed substantially by this change of binding energy. The effective binding energy scheme was not used in the final calculations, as it forces *a priori* decisions concerning the configuration of the state; also, no obviously consistent way of determining the effective binding energy to be used for a set of states was seen.

The momentum dependence, or nonlocality, of the optical potential can be treated by replacing the term

TABLE IV. Additional JULIE parameters. The three values of R_c are 12, 15, and 18 MeV results, respectively. The values of J^π in parentheses are uncertain as listed in *Nuclear Data Sheets*, May 1962.

J^π	E_{exc} (MeV)	l_j	N	BN (MeV)	Q (MeV)	R_c (F)
0^+	0	$(p)\frac{1}{2}$	1	5.0	15.63	3.0, 3.0, 3.0
2^+	4.43	$(p)\frac{3}{2}$	1	9.43	11.20	5.0, 5.0, 3.0
0^+	7.66	$(p)\frac{1}{2}$	1	12.66	7.97	5.0, 5.0, 2.0
3^-	9.64	$(d)\frac{5}{2}$	1	14.64	5.99	4.0, 4.0, 4.0
1^-	10.84	$[(s)\frac{1}{2}]$	(2)	15.84	4.79	3.0, 3.0, 3.0
(1^-)	11.83	$(s)\frac{1}{2}$	2	16.83	3.80	5.0, 2.0, 4.6
(1^+)	12.71	$(p)\frac{3}{2}$	1	17.71	2.92	5.0, 5.0, 5.0

$V(r)\Psi(\bar{r})$ in the Schrödinger equation by

$$\int V(\bar{r},\bar{r}')\Psi(\bar{r}')d\bar{r}',$$

where $V(\bar{r},\bar{r}')$ is the nonlocal potential. The reader is referred to the book of Hodgson[16] for a detailed treatment of this technique. The nonlocal potential is used in the calculation of the form factor for each transition, after being calculated using the iterative program FLANNEL FLURP. The calculation introduces a nonlocality into the real entrance-channel well, the bound-state well, and the real exit-channel well. The nonlocality ranges used were recommended by R. H. Bassel; they are empirically based. The nonlocal potential affected the shapes of the angular distributions little. However, the spectroscopic factors were changed considerably. With nonlocality, the ground-state spectroscopic factors increased by 10 to 50%. The excited-state spectroscopic factors decreased by 25 to 40%. The nonlocal potentials were used in the final analysis because it was felt that they should give better predictions than local potentials, since the inclusion of nonlocality is more realistic than the omission of these effects in the calculations.

It was necessary to use the lower cutoff version of the DWBA theory in order to get reasonable agreement between theory and experiment for the shapes of the angular distributions. The values of R_c (in F) used at 12.0, 15.0, and 18.0 MeV, respectively, are listed in Table IV. This table also lists several other parameters used in the JULIE calculations: l and j, the orbital and total angular momentum of the picked-up neutron; N, the neutron's radial quantum number; BN, neutron binding energy (here equal to its separation energy); Q, the reaction Q value in MeV.

In a normal DWBA calculation, the integration of the lth partial radial wave proceeds from some initial radius which is very small (compared to the nuclear radius) to an upper cutoff where the effects of the nuclear potential are no longer felt. A typical range of radial integration is from 0.05 to 20 F. However, in

[16] P. E. Hodgson, *The Optical Model of Elastic Scattering* (The Oxford Press, Oxford, 1963).

certain circumstances, it is found that the only way to get results agreeing in any way with the experiment is to employ a lower radial cutoff, R_c. In this case, the radial integration is done up to R_c, stored, and then completed up to the upper limit. The integral up to R_c is subtracted from the total. There is no general physical criterion for the choice of R_c. It has been found empirically that values of R_c roughly equal to the nuclear radius are the most successful. In fact, R_c is a free parameter, which can be adjusted to give the best agreement with the shape of the experimental angular distribution. The use of R_c tends to accentuate the relative contribution of the higher partial waves by suppressing the contributions in the nuclear interior which come primarily from lower partial waves. This is due to the presence of the centrifugal barrier term $l(l+1)/k^2r^2$ in the radial wave equation for u_l. Using a value of R_c close to the nuclear radius tends to reduce the calculated absolute cross section by a factor of order 5 to 30 over the case for $R_c=0$. Within the range $3\leqslant R_c\leqslant 5$ F the absolute cross section varies in an unpredictable manner by about a factor of 3. The consistency of our spectroscopic factors is somewhat surprising in view of that fact. If R_c is varied in steps of 0.2 F, the shapes and magnitudes of the angular distributions change smoothly and by small amounts. A variation of $\cong$0.5 F in R_c is needed to produce a significant change in the calculations.

Some theoretical justification for the use of cutoffs has been given recently by Buck and Rook.[17] They suggest that the use of R_c simulates the effect of coupling to other channels than those taken account of in usual DWBA calculations. They indicate that the effect of coupling to other channels is most important in cases where the difference between incoming and outgoing momenta is large, or when the reaction connects strongly and weakly absorbing channels. Both of these conditions appear to be met in the present reaction, and may be rather generally true in the (He^3,α) reaction for light nuclei.

j Dependence

The angular-distribution data show a pronounced j dependence. For $l=1$ pickup, the $p_{1/2}$ cases show much more pronounced oscillations than the $p_{3/2}$ cases, at c.m. angles between 90° and 180°. This effect has been seen previously in (d,p) reactions,[18] in (α,p) reactions,[19] and in the (He^3,α) reaction.[20]

There are several ways to introduce a corresponding j dependence into the DWBA calculations. One may introduce an $\mathbf{l}\cdot\mathbf{s}$ term into the entrance-channel elastic well, or the bound-neutron well, or the exit-channel well. In our case, we were already supplied with an $\mathbf{l}\cdot\mathbf{s}$ term in the entrance-channel well, which was required to fit the elastic data. We decided to restrict the use of $\mathbf{l}\cdot\mathbf{s}$ just to the entrance well, to keep the number of "free" parameters to a minimum. This procedure gave a j dependence in qualitative agreement with the measured data; i.e., the result for $j=l-\frac{1}{2}$ had more pronounced dips in the mid-range of angles than $j=l+\frac{1}{2}$ (Fig. 7). The final radial cutoffs used for the predictions shown here tend to obscure the consistency of the calculated j-dependence effect. If one follows the predictions through several values of R_c, the trend is clearer, however.

Spectroscopic Factor

The spectroscopic factor is defined by

$$\sigma(l,j)=NS(l,j)\sigma_{\text{JULIE}}(l,j)\ \text{mb/sr}, \qquad (1)$$

for the (He^3,α) reaction. The factor N depends, in part, on the overlap of the He^3 and alpha-particle wave functions and the strength of the interaction responsible for the transition. If one assumes that the wave function of the neutron relative to the ^{3}He ion is given by an exponential with wave number related to the neutron separation energy, one finds $N=1.63$.

The spectroscopic factors of all final states with a neutron hole in the (l,j) shell satisfy the sum rule

$$\sum_{J_F} S(l,j)=n, \qquad (2)$$

where n is the number of (l,j) neutrons in the target nucleus. The quantity $\sigma_{\text{JULIE}}(l,j)$ is that calculated by the JULIE code; $\sigma(l,j)$ would be equal to the experimental cross section if the DWBA calculations gave the right absolute cross section. In fact, the calculated value of $\sigma(l,j)$ is smaller than the experimental value, $\sigma_{\text{expt}}(l,j,E)$ by a large factor. Thus,

$$\sigma_{\text{expt}}(l,j,E)=K(E)\sigma(l,j). \qquad (3)$$

The values of $K(E)$ found here were 7.4, 6.3, and 4.4 at 12.0, 15.0, and 18.0 MeV, respectively.

The spectroscopic factors S quoted here (see Table V) are normalized so that $S=1$ for the ground state at each bombarding energy. A single value of S determined here is estimated to have a relative probable error of 50%. The values of S averaged over the three bombarding energies are denoted $\langle S\rangle$, and are estimated to have relative errors of 30%. Those for the 10.84-MeV state are less certain. This is due to the poorer agreement between the data and the DWBA calculations in that case, the larger statistical uncertainty in the data points, and the interference from oxygen contamination in the

[17] B. Buck and J. R. Rook, Nucl. Phys. **67**, 504 (1965).
[18] L. L. Lee, Jr., and J. P. Schiffer, Phys. Rev. Letters **12**, 108 (1964); L. L. Lee, Jr., and J. P. Schiffer, Phys. Rev. **136**, B405 (1964).
[19] L. L. Lee, Jr., A. Marinov, C. Mayer-Böricke, J. P. Schiffer, R. H. Bassel, R. M. Drisko, and G. R. Satchler, Phys. Rev. Letters **14**, 261 (1965).
[20] Claus Mayer-Böricke, R. H. Siemssen, and L. L. Lee, Jr., Bull. Am. Phys. Soc. **10**, 26 (1965).

TABLE V. The DWBA spectroscopic factors: S_{12} is $S(l,j,E)$, as defined in Eq. (1), for 12 MeV; S_{15} and S_{18} are the corresponding quantities at 15 and 18 MeV, respectively. The average of S over all three bombarding energies is denoted $\langle S\rangle$. The values of $K(E)$, defined in Eq. (3), were found to be 7.4 at 12 MeV, 6.3 at 15 MeV, and 4.4 at 18 MeV.

State	S_{12}	S_{15}	S_{18}	$\langle S\rangle$
Ground	1	1	1	1
4.433	0.34	0.64	1.57	0.85
7.656	0.067	0.083	0.082	0.077
9.64	0.10	0.19	0.11	0.13
10.84	(0.037)	(0.040)	(0.077)	(0.05)
11.83	0.062	0.045	0.075	0.06
12.71	0.75	2.31	2.49	1.85

target at the small forward angles. For these reasons, the values of S are parenthesized for that state.

CONCLUSIONS

The comparisons of the results of the DWBA calculation to the data in Fig. 5 show that the fits are poor at the lowest beam energy, 12 MeV. Some of them do, however, improve considerably at 15 MeV and are satisfactory at 18 MeV. There are at least two good reasons for this trend. The optical model works better at higher energies where no pronounced resonances in the elastic scattering occur. In this experiment the outgoing channel might still be somewhat affected by such resonances. Furthermore, the Born approximation is always better at high energies. It should be interesting to study this reaction at still higher energies where the agreement probably improves even further. In this work the best fits are obtained for the $l=1$ transition to the 12.71 state at 15 and 18 MeV. This transition is kinematically favored because at the nuclear surface the momentum transfer at forward angles corresponds approximately to the proper angular momentum transfer for $C^{13*}(l=1)$ as well as for $He^4(l=0)$. In the latter case, this simply means that the velocities of the incoming and outgoing light particle are nearly the same. The cross section is, therefore, quite large and other reaction mechanisms, such as compound-nuclear reaction and heavy particle stripping, are negligible. In addition, the energy of the outgoing alpha particle (Q value 2.92 MeV) is not far from 17 MeV, where the α-110 optical-model parameters were obtained.

The Ground-State (He^3,α) Transition

The ground state of C^{13} would have a configuration $s_{1/2}{}^4p_{3/2}{}^8p_{1/2}$ in the jj-coupling shell model. Previous arguments have been given for jj-coupling in C^{12} by French.[21] On this assumption, the spectroscopic factor is normalized to unity for this state, since there is one neutron available for pickup. The DWBA calculation assuming $p_{1/2}$ pickup gave the best agreement with the data in this case as well.

[21] J. B. French, in *Nuclear Spectroscopy, Part B*, edited by F. Ajzenberg-Selove (Academic Press Inc., New York, 1960).

The 4.433-MeV, 2^+ and 12.71-MeV, 1^+ States

The states formed by pickup of a $p_{3/2}$ neutron can have spin and parity 2^+ or 1^+. The sum of the spectroscopic factors for all such states should be four. The observed sum is 2.5 ± 0.75 or $60\%\pm18\%$ of the single-particle strength for such transitions. The larger spectroscopic factor for the 1^+ state is understandable in view of its proximity to the particle-hole excitation energy for a $p_{3/2}{}^{-1}p_{1/2}$ configuration in C^{12}, which was obtained by Vinh-Mau and Brown[22] as $\cong$13.8 MeV.

Presumably, some of the single-particle strength for $p_{3/2}$ pickup would go to the 15.11 MeV, $1^+(T=1)$ state in C^{12}, which was not measured in this experiment.

The ratio of spectroscopic factors of the 4.433-MeV state to the ground state of 0.85 found in our experiment agrees within experimental errors with that of 0.97 found by Bennett[1] from his study of the $C^{13}(p,d)C^{12}$ reaction, and of 0.76 found by Mayo and Hamburger[23] from their work on the $C^{13}(d,t)C^{12}$ reaction. Desphande[6] obtained a value of 1.29 from the $C^{13}(He^3,\alpha)C^{12}$ reaction at energies up to 10.29 MeV. He did a DWBA analysis, but did not have reliable optical parameters available for the entrance channel. It should be mentioned also that our value for the ratio would have been in better agreement with Deshpande's (and poorer agreement with the other work), had we not included nonlocality effects.

The 7.656-MeV, 0^+ and 9.64-MeV, 3^- States

The transition to the 3^- state is excited more strongly than would be expected on a simple shell-model picture. The poor agreement with DWBA might indicate a sizeable contribution from another reaction mechanism such as compound-nuclear reaction. The lack of structure in the measured angular distribution could be construed as supporting this assumption. However, let us consider the evidence supporting the hypothesis that this is a direct transition. The only way a 3^- state could be formed directly is by $l=2$ or higher. An $l=2$ direct pickup is expected to have a rather broad first maximum in the angular distribution, whose position moves toward smaller angles with increasing bombarding energy. This feature is seen clearly in the data for the 9.64-MeV state. This leads to the conclusion that the ground state of C^{13} contains some $d_{5/2}$ particles. The only reasonable configuration that has the same parity as the C^{13} ground state is known to have would be $p_{3/2}{}^{-2}d_{5/2}{}^2p_{1/2}$. This immediately provides an explanation for the 7.656 MeV, 0^+ state as being formed by the pickup of the $p_{1/2}$ neutron from this configuration.[24] The 3^- state should be approximately twice

[22] N. Vinh-Mau. and G. E. Brown, Nucl. Phys. **29**, 89 (1962).
[23] S. Mayo and A. I. Hamburger, Phys. Rev. **117**, 832 (1960).
[24] See D. Hasselgren, P. U. Renberg, O. Sundberg, and G. Tibell, Phys. Letters **9**, 166 (1964); and L. I. Schiff, Phys. Rev. **98**, 1281 (1955) for pertinent discussion of this state.

as strong as the 0^+ state on this assumption, due to the number of available neutrons. The experimental ratio of spectroscopic factors is 1.75 ± 0.45, which agrees within the limits of error.

If the ground state of C^{13} were deformed, the presence of a $d_{5/2}^2$ configuration would not be so surprising. For values of Nilsson's deformation parameter $\delta>0.3$, the $K=\frac{1}{2}$ member of the $d_{5/2}$ band is brought down quite far from the level at $\delta=0$; practically degenerate with the $p_{1/2}$ level.[25]

The 10.84 MeV, 1^- and 11.83 MeV, (1^-) States

Both of these states are excited by $s_{1/2}$ pickup, and are wide. The agreement with the DWBA predictions was poor for the 10.84 MeV state, but $l=0$ gave the best fit. One possible reason for the failure of DWBA for these two states lies in their short lifetime which is of the same order of magnitude as the interaction time.

It seems improbable that these states would be formed by pickup of a $1s_{1/2}$ neutron, since the corresponding particle-hole excitation energy found by Vinh-Mau and Brown[22] is 31 MeV. It appears more likely that these states are excited through a configuration of the type $p_{3/2}^{-2}\,2s_{1/2}^2p_{1/2}$.

[25] S. G. Nilsson and B. R. Mottelson, Kgl. Danske Vidensk Selskab, Mat. Fys. Skrifter 1, No. 8 (1959).

ACKNOWLEDGMENTS

We would like to express our appreciation for the assistance rendered by Dr. R. H. Bassel and the Oak Ridge National Laboratory in obtaining the optical-model fits and the DWBA predictions. We are also grateful to Dr. C. M. Fou for help in data-taking and analysis. James Joyce and William Focht, as well as the operating staff of the Tandem Accelerator Laboratory, deserve mention for their help in obtaining the data.

PHYSICAL REVIEW VOLUME 152, NUMBER 3 16 DECEMBER 1966

Excitation of Generalized Giant Collective Multipole States by Electron Scattering

R. RAPHAEL AND H. ÜBERALL*
Physics Department, The Catholic University, Washington, D. C.

AND

CARL WERNTZ†
Physics Department, The Catholic University, Washington, D. C.
and
U. S. Naval Ordnance Laboratory, White Oak, Maryland

(Received 31 May 1966; revised manuscript received 28 July 1966)

A new collective model for finite nuclei is presented which treats all of the four types of excitations of nuclear matter in arbitrary orbital-angular-momentum states. The model avoids the normal assumption of a constant ground-state density by generating the collective motion through a coordinate-scale-factor transformation of the ground-state density distribution. The cross sections for excitation of these generalized collective states by inelastic electron scattering are calculated for monopole and quadrupole oscillations. A specific application to the 180° inelastic scattering of electrons from ^{16}O is given. It is shown that the model exhausts the corresponding multipole sum rules.

I. INTRODUCTION

THE nuclear photoeffect is strikingly dominated[1] by the giant electric dipole resonance which was first described by Goldhaber and Teller[2] as a dipole oscillation of the protons as a whole against the neutrons as a whole in the nucleus. If one considers nuclear matter as made up of four interacting fluids, spin-up and -down protons and spin-up and -down neutrons, three other types of "normal modes" are possible.[3] These three are the *compressional mode*, all four fluids in phase, the *spin mode*, spin-up nucleons against spin-down nucleons, and the *spin-isospin* mode, spin-up protons and spin-down neutrons against the other two fluids. Following this nomenclature, we shall designate the Goldhaber-Teller mode as the *isospin* mode.

A phenomenological quantized oscillator model of the

* Supported in part by a grant from the U. S. National Science Foundation.
† Supported in part by a grant from the U. S. Air Force Office of Scientific Research.

[1] E. Hayward, Rev. Mod. Phys. 35, 324 (1963).
[2] M. Goldhaber and E. Teller, Phys. Rev. 74, 1046 (1948).
[3] W. Wild, Bayr. Akad. Wiss. Mat.-Naturw. Klasse 18, 371 (1956); S. Fallieros, R. A. Ferrell, and M. K. Pal, Nucl. Phys. 15, 363 (1960); A. E. Glassgold, W. Heckrotte, and K. M. Watson, Ann. Phys. (N. Y.) 6, 1 (1959).